Confocal Arthroscopic Assessment of Osteoarthritis In Situ

Daniel Smolinski, B.Eng., Chris W. Jones, B.Eng.,
Jian P. Wu, M.Eng, Karol Miller, Ph.D., D.Sc., Thomas B. Kirk, Ph.D.,
and Ming H. Zheng, Ph.D., D.M., F.R.C.Path.

Purpose: This study aimed to assess the ability of the laser scanning confocal arthroscope (LSCA) to evaluate cartilage microstructure, particularly in differentiating stages of human osteoarthritis (OA) as classified by the International Cartilage Repair Society (ICRS) OA grade definitions. **Methods:** Ten tibial plateaus from total knee arthroplasty patients were obtained at the time of surgery. Cartilage areas were visually graded based on the ICRS classification, imaged by use of a 7-mm-diameter LSCA (488-nm excitation with 0.5% [wt/vol] fluorescein, 20-minute staining period), and then removed with underlying bone for histologic examination with H&E staining. The 2 imaging techniques were then compared for each ICRS grade to ascertain similarity between the methods and thus gauge the techniques' diagnostic resolution. Cartilage surface degeneration was readily imaged and OA severity accurately gauged by the LSCA and confirmed by histology. **Results:** LSCA and histologic images of specimens in the late stages of OA were seen to be mutually related even though they were imaged in planes that were orthogonal to each other. Useful and comparable diagnostic resolution was obtained in all imaged specimens from subjects with various stages of OA. **Conclusions:** This study showed the LSCA's ability to image detailed cartilage surface morphologic features that identify grade 1 through 4 of the ICRS OA grading system. The LSCA's imaging potential was best shown by its ability to resolve the fine collagen network present under the lamina splendens. The incorporation of high-magnification confocal technology within the confines of an arthroscopic probe has proved to provide the imaging requirements necessary to perform detailed cartilage condition assessment. **Clinical Relevance:** In comparison to video arthroscopy, LSCA provides increased magnification along with improved contrast and resolution. **Key Words:** Osteoarthritis—Human knee—Confocal arthroscopy—In situ.

Osteoarthritis (OA) is a slow-progression syndrome[1] that degrades cartilage structure to the point where it can no longer support the loads applied to it. The etiology of OA is still not well understood,[2] and early diagnosis is still very difficult to provide.[3] Early-stage OA diagnosis is critical if long-term disability is to be reduced through treatment, education, and lifestyle change.[4,5]

The laser scanning confocal arthroscope (LSCA) was developed to address the low imaging resolution of current cartilage OA assessment technologies such as magnetic resonance imaging and radiography. By developing an OA diagnostic method capable of investigating tissue morphology in vivo, it is hoped that increased sensitivity and consistency in cartilage condition diagnosis can be gained. The LSCA works on the same principle as a bench-top confocal system, the difference being the unique miniaturized laser scanning mechanism.[6,7] It thus offers the same advantages offered by confocal microscopy such as high-resolution, high-contrast, fully focused images as a result of

From the School of Mechanical Engineering (D.S., C.W.J., J.P.W., K.M., T.B.K.) and .School of Pathology and Surgery, Department of Orthopaedics (C.W.J., M.H.Z.), University of Western Australia, Perth, Australia.

Supported by a SPRIT Grant from the Australian Research Council (project ID No. C00107367). Financial support was also provided by the University of Western Australia and the Julian Hunka Memorial Trust. The authors report no conflict of interest.

Address correspondence and reprints requests to Thomas B. Kirk, Ph.D., School of Mechanical Engineering, MPD 50, University of Western Australia, 35 Stirling Hwy, Crawley WA 6009, Australia. E-mail: kirk@cyllene.uwa.edu.au

0749-8063/08/2404-6439$34.00/0
doi:10.1016/j.arthro.2007.10.003

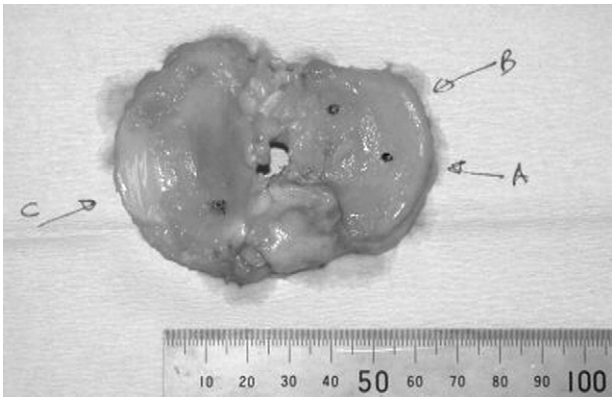

FIGURE 1. Image of contrasting agent–stained tibial plateau. Marked areas (A, B, and C) represent various ICRS OA grades, which were graded en face before being imaged with the LSCA.

a simple out-of-focus light-rejection method.[8,9] Confocal imaging achieves out-of-focus light rejection by use of 2 techniques: (1) the minimization of the total illuminated tissue volume through the use of highly focused lenses and (2) the attenuation of light outside the expected "focused" return light path by the utilization of a pre-detector aperture. Previous studies have highlighted the fact that the diagnostic sensitivity of an instrument depends on image contrast and spatial resolution.[10] By providing both of these features, the LSCA has the potential to aid in the assessment of cartilage condition, as well as cartilage repair techniques, by facilitating the imaging of finer anatomic changes.

This study aimed to assess the developed LSCA's OA diagnostic capability for possible future in vivo application. It aims to prove the hypothesis that the LSCA instrument is capable of equal sensitivity to the currently used OA diagnosis method based on the OA grading system of the International Cartilage Repair Society (ICRS).[11]

METHODS

Specimens

Ten human tibial plateaus were acquired from total knee arthroplasty surgeries when convenient to the surgeon, with the approval of the human ethics committee. The minimum and maximum ages of the patients from whom cartilage was obtained were 54 and 86 years, respectively, with a mean of 74 years. Only tissue from healthy patients was accepted into the study, thus eliminating any risk of infection. Topographic regions of the tibial plateaus to be imaged were selected on the basis of their OA progression (1 site per ICRS OA grade selected on each tibial plateau), not the specific location (Fig 1).

Sample Preparation

To minimize dehydration, samples (once collected from the operating theatre) were covered with moistened (0.9% [wt/vol] saline solution) paper towels and stored in 50-mL sealed plastic sample containers in a cold room (−4°C) until being imaged within 24 hours of sample acquisition. Specimen storage at −4°C was necessary because the time between sample collection and imaging was governed by LSCA equipment availability.

Assessment of ICRS OA Grade

Once the samples thawed, OA severity was gauged by use of the ICRS OA grading scale,[11] which has been proven to be accurate and repeatable.[12] ICRS OA grading was used in this study as the OA severity guide in performing a double comparison between LSCA and histologic imaging. Areas were examined

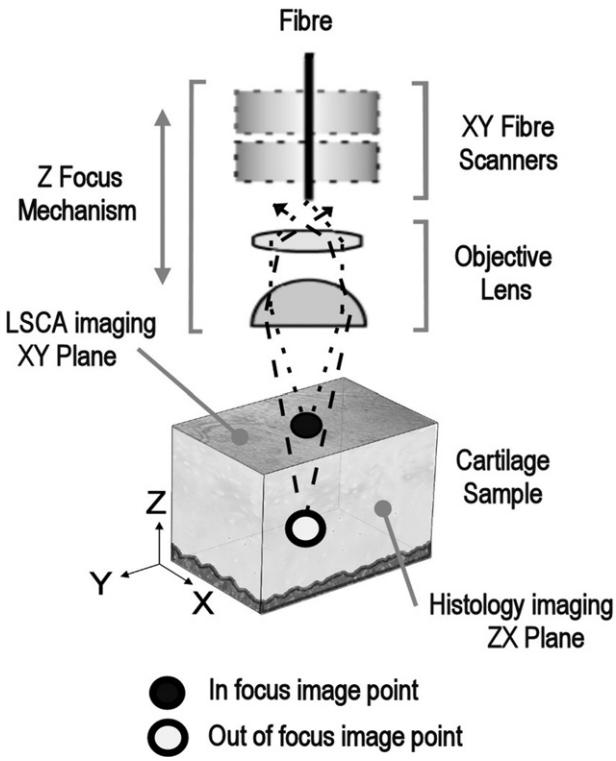

FIGURE 2. LSCA's out-of-focus light rejection principle schematic along with imaging plane perspective for both confocal and histologic images.

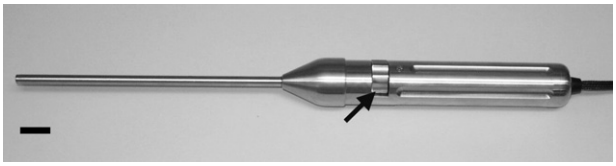

FIGURE 3. LSCA used in study, featuring an imaging tip with a 7-mm outside diameter (scale bar, 20 mm). The arrow shows the focal plane depth selector dial.

and assessed en face by 2 of the investigators with the help of tweezers to gauge cartilage tissue hardness and fibrillation. The area under consideration was deemed to be of a particular ICRS OA grade only if both cartilage examiners concurred. Selected areas were marked with a grease-proof marker (UniMarker; Mitsubishi Pencil, Tokyo, Japan) and digitally photographed (3.1 megapixels).

LSCA System

The LSCA uses a focused laser light source to illuminate a small volume within the specimen (Fig 2). The incident laser light excites the previously applied contrasting agent in the tissue, emitting a longer wavelength. Returned light detection occurs along the same optical path before being filtered by a long pass filter, which only lets light through over a particular wavelength into a photodetector. Out-of-focus light rejection in the LSCA setup is achieved by use of the launch fiber end as the detector confocal aperture. The returned light, which in a bright-field microscope would generate a progressively increasing out-of-focus image signal, thus generates very little image noise in a confocal system. By raster scanning (scanned series of horizontal lines from top to bottom) of the single excitation point, a fully in-focus image is thus created. The current LSCA provides a spatial resolution$_{XY}$ of 2 μm, with an image refresh rate of 2 Hz.

Confocal Arthroscopy

Tibial plateaus were immersed in the contrasting agent (0.5% [wt/vol] fluorescein; Pharmalab, Brookvale, Australia) for 20 minutes. Once removed, they were thoroughly irrigated (0.9% [wt/vol] saline solution) to remove excess stain. The previously ICRS OA–graded and marked areas of interest were then imaged by placing the end of the LSCA probe perpendicular to the cartilage surface. The area was continuously irrigated with saline solution to keep the cartilage hydrated and the LSCA tip immersed, thus avoiding air bubbles.

The LSCA probe (Fig 3) used had an outer diameter of 7.0 mm, with 30× magnification, which corresponded to a field of view of 200 × 200 μm (512 × 512 pixels). The excitation wavelength used was 488 nm (argon ion laser) with the excitation laser power at the tip equal to 1.5 mW. The return signal was detected by use of a 515-nm long pass filter. Black level and gain settings were adjusted to provide optimum image quality without pixel saturation.

Histologic Preparation

After LSCA imaging, areas of interest were removed in 8 × 8–mm blocks with a chisel and mallet, with the subchondral bone trimmed to approximately 1 mm in thickness. Personal safety equipment was used during all sample contact. Care was taken to cut the cartilage samples so that the LSCA-imaged area remained in the center of the block. This ensured that when midsections were histologically imaged, the central area matched the previously LSCA-imaged region. The samples were fixed in 10% buffered formol saline solution for 2 weeks and rinsed with saline solution (0.9% [wt/vol]) before being decalcified twice (with no rinsing in between) in 15% (vol/vol) formic acid/sodium formate until soft enough for sectioning. After paraffin embedding, each block was bisected along the XY-plane centerline from which an XZ section was taken for pathology. H&E was used for bright-field histologic imaging performed with an Olympus DP11-P digital head mounted on an Olympus BX50 microscope with a UPlanFl 20x/0.50 numerical aperture objective (Olympus, Center Valley, PA).

RESULTS

In total 40 confocal image sets (10 per ICRS OA grade) were acquired, with each of the 10 tibial plateaus providing OA grades from 1 through 4. Only the best 2 confocal images (in terms of detail and contrast) from each ICRS OA grade are presented, along with the LSCA-imaged area's corresponding histologically imaged area. Images from the LSCA are represented at full field of view (200 × 200 μm), whereas the histologic images were cropped to match the LSCA's magnification and field of view to facilitate effortless comparison between morphologic features. It is important to note that the LSCA images were taken parallel to the cartilage surface (XY plane) whereas

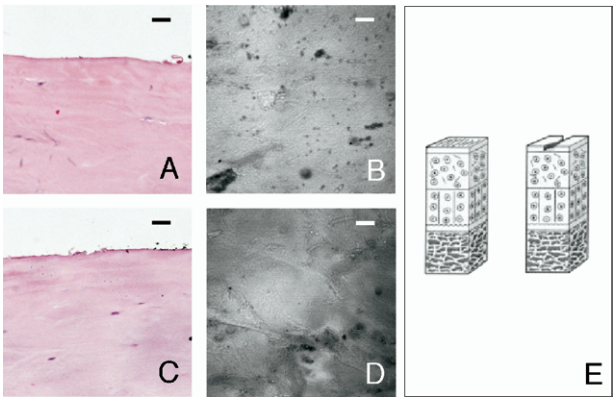

FIGURE 4. ICRS OA grade 1 specimens (scale bar, 20 μm). (A, C) H&E-stained histologic images (XZ plane). (B, D) LSCA images (XY plane) of corresponding sample. (E) Corresponding ICRS OA grade diagram. (Published with kind permission from ICRS—International Cartilage Repair Society.[11])

the histologic images were obtained perpendicular to the cartilage surface in the XZ plane (Fig 2). Variations in LSCA image brightness should not be interpreted as stain uptake because the photomultiplier tube's black level and gain were not kept constant but were adjusted to give an optimal image.

ICRS OA Grade 1

ICRS OA grade 1 was distinguished en face by the articular cartilage's firm feel and dull yellowish appearance. Under confocal examination, the cartilage surface texture appeared to be relatively free from unevenness and fibrillation, which occur in later stages of OA. Figure 4A and its corresponding confocal image (Fig 4B) show that the surface possesses a virtually smooth articular surface. The presence of fine collagen bundles in Figure 4B suggests that the lamina splenda, which is devoid of collagen fibers,[13] has been breached, indicating that this is ICRS OA grade 1 cartilage. Chondrocytes that are present on histologic analysis are spindle-shaped, which is typical of the superficial zone. Small dark areas (approximately 20 μm in diameter) visible on the confocal images, especially Figure 4B, are nonfluorescent ink particles from the marking pen used to denote areas of interest. The LSCA image in Figure 4D shows slight collagen matrix disruption, evidenced by surface texture undulations. The corresponding histologic image is smooth and lacking any fibrillation as expected for this OA grade.

ICRS OA Grade 2

On physical examination, ICRS OA grade 2 cartilage appeared intact, although slight softness was detected on physical probing. The main surface features present on the confocal images are the matted collagen bundles of 2 μm in diameter. Inter-territorial matrix collagen fibers of 300 nm in diameter, usually present in this zone,[14] most likely adhered together as a result of OA-induced proteoglycan depletion. The appearance of oblique clefts on the histologic images confirms that this is the middle zone. The middle zone's obliquely oriented collagen fibers are in transition between the tangentially oriented collagen of the surface zone and the deeper zone's perpendicularly oriented collagen fibers, thus showing that the imaged cartilage is indeed ICRS OA grade 2 cartilage, as represented in Figure 5E. Figure 5A shows slight surface fibrillation along with chondrocyte depletion, indicating advanced OA degeneration of the tissue. Figure 5C and D shows cartilage surface unevenness, with the confocal image showing randomized collagen bundles. The collagen bundles appear to be becoming separated from the surface compared with the previous ICRS OA grade. The collagen bundles also appear to be quite disorganized and lacking anisotropy, which has previously been found to be a feature of the middle zone.[15]

ICRS OA Grade 3

On physical inspection of ICRS OA grade 3 cartilage, it appeared frayed and much softer (chondromalacia) than normal. Histologic images from

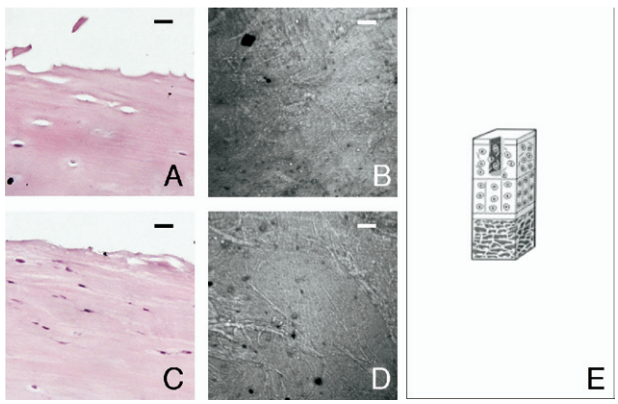

FIGURE 5. ICRS OA grade 2 specimens (scale bar, 20 μm). (A, C) H&E-stained histologic images (XZ plane). (B, D) LSCA images (XY plane) of corresponding sample. (E) Corresponding ICRS OA grade diagram. (Published with kind permission from ICRS—International Cartilage Repair Society.[11])

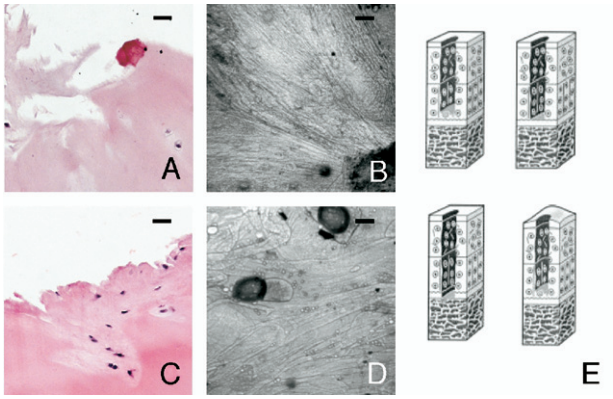

FIGURE 6. ICRS OA grade 3 specimens (scale bar, 20 μm). (A, C) H&E-stained histologic images (XZ plane). (B, D) LSCA images (XY plane) of corresponding sample. (E) Corresponding ICRS OA grade diagram. (Published with kind permission from ICRS—International Cartilage Repair Society.[11])

these cartilage areas show an increasingly fibrillated surface (Fig 6A and C). The advanced breakdown of cartilage is also evident from the reduced numbers of chondrocytes present in the tissue resulting from their necrosis (Fig 6C). Cartilage fibrillation on the confocal images shows up as layered sheets. This layered appearance is formed as vertical cartilage clefts formed by the fibrillation of the cartilage's deep zone press up against the LSCA's tip (Fig 6B and D). Frayed cartilage has previously been imaged en face in the XY plane by use of scanning electron microscopy, and the resulting images possessed a similar appearance, which was described as cartilage "flow."[16] Figure 6C shows fibroblasts in the matrix, suggesting that the lighter H&E-stained tissue is fibrocartilage repair tissue. The 2 approximately 20-μm-diameter circular objects in Figure 7D are imaging aberrations that manifested as a result of moisture penetration of the LSCA imaging window seal.

ICRS OA Grade 4

Physical inspection of ICRS OA grade 4 cartilage showed a hard bone mass with fine grooves along the direction of knee articulation. Figure 7A and B shows severely worn calcified cartilage. The confocal image shows cartilage exhibiting micro-cracks caused by the increased brittleness of the cartilage in this zone. The tissue, once having undergone eburnation to this extent, becomes a well-polished ivory mass–like surface. Fully degraded cartilage is shown in Figure 7C and D, where the subchondral bone has become exposed. The confocal image (Fig 7D) presents easily visible trabeculae and osteocytes, which are expected once the osteochondral junction has been penetrated. The concentric lamellae that surround the haversian canal are also well visualized.

DISCUSSION

The main finding of this study was that the LSCA is capable of producing real-time micro-level morphologic imaging, allowing for easy cartilage surface condition assessment and thus providing an indication of OA progression. From the presented images, it can be seen that the confocal gross morphology features observed are akin to the histologic findings of respective ICRS OA grades, though taken in orthogonal planes. Although the LSCA did not produce cartilage tissue morphology images under the OA-deteriorated cartilage surface, the images did provide a demonstration of the instrument's capability in cartilage surface texture imaging, which itself is an indication of cartilage condition. The study shows that cartilage surface appearance, which is normally qualitatively classified by optical arthroscopy,[17] can now be viewed with higher resolution, thus providing more information to the investigator trying to ascertain cartilage OA grade.

Although the study only yielded subjective diagnostic information, it can be seen in Figure 4 that collagen disruption is more clearly evident on the confocal images than on the equivalent histologic images. This is an important advantage, because the first observed

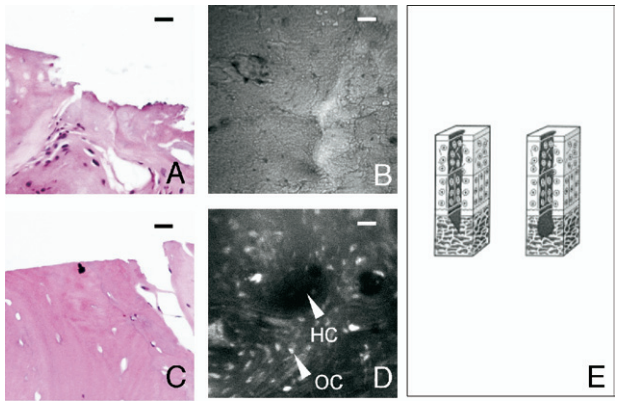

FIGURE 7. ICRS OA grade 4 specimens (scale bar, 20 μm). (A, C) H&E-stained histologic images (XZ plane). (B, D) LSCA images (XY plane) of corresponding sample. Subchondral bone with osteocytes (OC) and haversian canal (HC) within concentric lamellae is visible. (E) Corresponding ICRS OA grade diagram. (Published with kind permission from ICRS—International Cartilage Repair Society.[11])

change in cartilage due to OA is surface fibrillation.[5] Strong similarities were observed between the confocal and histologic images, with image sets displaying nearly identical morphologic surface features of the sampled areas. Although the LSCA's diagnostic resolution was not quantitatively measured, confocal images for ICRS OA grades 1 to 4 show distinct differences compared with each other, including collagen fiber organization, cartilage fibrillation, and the presence of subchondral bone. This showed that the LSCA's diagnostic resolution is capable of determining the OA grade with resolution equal to that of the ICRS grading system.

The LSCA can be compared with other emerging, novel arthroscopic cartilage imaging techniques, such as optical coherence tomography (OCT), which is also used for cartilage injury and OA assessment.[18,19] The LSCA provides XY-plane images, whereas the OCT imaging technique images in the ZX plane used in histologic studies of cartilage. OCT images are acquired to a depth of 1 to 1.5 mm, with a spatial resolution of 4 to 20 μm.[18] In contrast, the LSCA used in this study possessed a spatial resolution of 2 μm, thus surpassing OCT's "ultrahigh resolution" mentioned by Herrmann et al.[19] OCT does possess a much higher tissue penetration than the LSCA that, when previously tested on bovine cartilage tissue, provided images to a depth of 200 μm before signal attenuation became a problem. OCT with its current resolution and imaging plane is a good tool for cartilage thickness measurement as shown by Herrmann et al., who gained cartilage thickness values within 7% to 9% of those gained by histologic methods. In comparison, the imaging plane and high resolution of the LSCA allow the operator to view increased cartilage detail of morphologic features that are already familiar to the him or her, making the use of the LSCA very intuitive with minimal training.

In this study we did not image healthy human cartilage (ICRS OA grade 0) due to the cartilage samples being collected at convenience and the difficulty of obtaining healthy human cartilage. Although the most difficult to obtain, human cartilage was chosen as the most suitable tissue to study because it is important to build up an image database for clinicians to become familiarized with this imaging technique if it is to be used for diagnosis. A further limitation of this study results from the inability to guarantee the imaging of the exact same area by use of the 2 imaging modalities under comparison. The LSCA possesses a field of view of 200 $\times$ 200 μm, which is very difficult to re-locate in histologic images of the same cartilage sample. We endeavored, to the best of our ability, to image and provide identical cartilage sample areas for comparison by performing careful cartilage sample removal and histologic slide preparation. Histologic comparison images were taken as close to the center of the histology sections as possible (i.e., from the mid block) to try to represent the LSCA-imaged area as closely as possible.

The limited tissue penetration of the contrasting agent was not foreseen, because previous imaging of in situ animal cartilage provided good imaging penetration (approximately 200 μm) after the same period and conditions ex vivo. This presented an issue because contrasting agent penetration is the main challenge in acquiring good confocal images.[20] The low stain penetration could have been attributed to tissue dehydration, which was actively being minimized during the study. Another explanation could be the age of the tissue itself, because it is known that tissue hydration is reduced with age.[21] The reason will have to be investigated further if future studies are to be carried out on aged human cartilage.

CONCLUSIONS

This study showed the LSCA's ability to image detailed cartilage surface morphologic features that identify grades 1 through 4 of the ICRS OA grading system. The LSCA's imaging potential was best shown by its ability to resolve the fine collagen network present under the lamina splendens. The incorporation of high-magnification confocal technology within the confines of an arthroscopic probe provides the imaging requirements necessary to perform detailed cartilage condition assessment.

Acknowledgment: The authors are grateful for the equipment supplied by OptiScan (Victoria, Australia). They also thank Professor David Wood and Dr. Lawrence O'Hara for their help in obtaining the human osteochondral samples used in this study.

REFERENCES

1. Gardner DL, Salter DM, Oates K. Advances in the microscopy of osteoarthritis. *Microsc Res Tech* 1997;37:245-270.
2. Adams ME, Wallace CJ. Quantitative imaging of osteoarthritis. *Semin Arthritis Rheum* 1991;20:26-39 (suppl 2).
3. Hammad TA. Structure modification in knee osteoarthritis: Methodology and outcome parameters. *Osteoarthritis Cartilage* 2001;9:488-498.
4. The bone and joint decade 2000-2010. *Osteoarthritis Cartilage* 1999;7:251-254.
5. Chiang EH, Laing TJ, Meyer CR, Boes JL, Rubin JM, Adler

RS. Ultrasonic characterization of in vitro osteoarthritic articular cartilage with validation by confocal microscopy. *Ultrasound Med Biol* 1997;23:205-213.
6. Delaney PM, Harris MR, King RG. Fibre-optic laser scanning confocal microscopy suitable for fluorescence imaging. *Appl Opt* 1994;33:573-577.
7. Delaney PM, Harris MR, King RG. Novel microscopy using fibre optic confocal imaging and its suitability for subsurface blood vessel imaging in vivo. *Clin Exp Pharmacol Physiol* 1993;20:197-198.
8. Harvath L. Overview of fluorescence analysis with confocal microscope. *Methods Mol Biol* 1999;115:149-158.
9. Dailey M, Marrs G, Satz J, Waite M. Concepts in imaging and microscopy. Exploring biological structure and function with confocal microscopy. *Biol Bull* 1999;197:115-122.
10. Buckland-Wright JC. Current status of imaging procedures in the diagnosis, prognosis and monitoring of osteoarthritis. *Baillieres Clin Rheumatol* 1997;11:727-748.
11. ICRS cartilage injury evaluation package. Zollikon, Switzerland: International Cartilage Repair Society, 2000.
12. Smith GD, Taylor J, Almqvist KF, et al. Arthroscopic assessment of cartilage repair: A validation study of 2 scoring systems. *Arthroscopy* 2005;21:1462-1467.
13. Jeffery AK, Blunn GW, Archer CW, Bentley G. Three-dimensional collagen architecture in bovine articular cartilage. *J Bone Joint Surg Br* 1991;73:795-801.
14. Schenk RK, Eggli PS, Hunziker EB. *Articular cartilage morphology*. In: Kuettner KE, Schleyervach R, Hascall VC. Articular cartilage biochemistry. New York: Raven, 1986;3-20.
15. Goodwin DW, Zhu H, Dunn JF. In vitro MR imaging of hyaline cartilage: Correlation with scanning electron microscopy. *AJR Am J Roentgenol* 2000;174:405-409.
16. Ghadially FN, Ailsby RL, Oryschak AF. Scanning electron microscopy of superficial defects in articular cartilage. *Ann Rheum Dis* 1974;33:327.
17. Hjelle K, Solheim E, Strand T, Muri R, Brittberg M. Articular cartilage defects in 1,000 knee arthroscopies. *Arthroscopy* 2002;18:730-734.
18. Chu CR, Lin D, Geisler JL, Chu CT, Fu FH, Pan Y. Arthroscopic microscopy of articular cartilage using optical coherence tomography. *Am J Sports Med* 2004;32:699-709.
19. Herrmann JM, Pitris C, Bouma BE, et al. High resolution imaging of normal and osteoarthritic cartilage with optical coherence tomography. *J Rheumatol* 1999;26:627-635.
20. Tsien RY, Waggoner A. Fluorophores for confocal microscopy: Photophysics and photochemistry. In: Pawley J, ed. *Handbook of biological confocal microscopy*. New York: Plenum, 1990;169-178.
21. Venn MF. Variation of chemical composition with age in human femoral head cartilage. *Ann Rheum Dis* 1978;37:168-174.